

# *In situ* imaging of polymer melt spreading with a high-temperature atomic force microscope

D. Glick, P. Thiansathaporn, and R. Superfine<sup>a)</sup>

Department of Physics and Astronomy, University of North Carolina at Chapel Hill, Chapel Hill, North Carolina 27599

(Received 9 June 1997; accepted for publication 16 October 1997)

We have developed a method of imaging at high temperatures with atomic force microscopy using a laser to deliver heat to an area localized around the AFM tip-sample junction. We couple approximately 75 mW from an argon-ion laser into the active region to raise the temperature of a 100 nm gold film to around 225 °C. As a sample, we use 1.2  $\mu\text{m}$  polystyrene spheres adsorbed onto the film. We image the flow of these spheres, *in situ*, over the course of an hour. The dynamics of the polymer spreading is shown to be consistent with the dry spreading of a precursor film. © 1997 American Institute of Physics. [S0003-6951(97)03750-9]

The field of scanning probe microscopy has become firmly established over the past ten years in a broad range of fundamental science and industrial applications. In its many forms, atomic force microscopy (AFM) allows the quantitative study of topography, compliance, adhesion, and friction, all correlated on the nanometer length scale.<sup>1</sup> While the vast majority of the AFM work has been done at room temperature, there are many applications that could exploit the abilities of AFM if experiments could be performed at high temperatures. For industrial concerns, there is a clear need for versatile analytical techniques, which can be applied *in situ* to elucidate complex materials processing. In this letter, we present our work in successful AFM imaging of delicate samples at elevated temperatures of about 225 °C. We describe our technique for local sample heating using laser illumination and its application to polymer melt flow.

The flow of polymers in the melt is of great interest to basic science and appears in many industrial processes including coatings, injection molding, and adhesives. During these processing steps, the polymer temperature is raised well above the glass transition temperature ( $T_g$ ). There has been a great deal of interest in liquid and polymer flow over surfaces, and many features of the spreading of low molecular weight liquids on smooth surfaces have been explored both through theory and experiments.<sup>2</sup> Previous studies that have employed scanning electron microscopy or ellipsometry sacrifice either quantitative topography or lateral resolution.<sup>3</sup> Atomic force microscopy can provide the surface topography with nanometer resolution in all three coordinates, as well as provide chemical specificity. The challenge lies in making AFM an *in situ* tool. The dominant problem in high-temperature AFM (HT-AFM) is drift in the sample position or cantilever deflection.<sup>4</sup> We have circumvented this problem by using a laser as a heat source.<sup>5</sup> Laser illumination can be focused down to the length scale of microns, isolating heat deposition to the scan area. In addition to lateral isolation, we have employed the total internal reflection geometry in order to minimize the direct laser heating of the AFM tip or cantilever.

We have used a modified Digital Instruments, Inc. Nanoscope III as the AFM in this experiment. A 514 nm argon laser was used as the light source providing an input power of 75 mW. We deposited 1.2  $\mu\text{m}$  polystyrene beads ( $M_w = 250\text{--}1000$  kg/mol) with distilled water solution onto a lithographically patterned 100 nm gold film (with a 2 nm chromium underlayer) evaporated onto a BK7 glass prism. The sample was then placed in an oven at 100 °C for 10 min in order to establish initial adhesion between the beads and the substrate. The laser ( $d \sim 100$   $\mu\text{m}$ ) was coupled into the metal film using the total internal reflection geometry (Fig. 1). Imaging was done at an elevated temperature using high amplitude resonance techniques with a silicon cantilever ( $\omega = 158$  kHz,  $k \approx 50$  N/m) and tip.

For this experiment, the AFM tip was positioned over an area at the corner of the gold film where several balls were adsorbed. The laser was focused near this location; the center of the beam offset by  $\sim 25$   $\mu\text{m}$  to the lower left. Figure 2 shows a group of four spheres with AFM images selected at 20 min intervals. The spheres toward the top of the image, away from the laser, were cooler, and showed a slower spreading rate. The noninvasive nature of the high-temperature imaging was tested by imaging individual

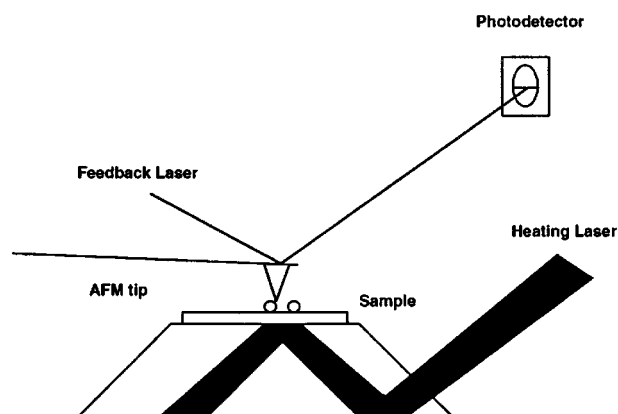


FIG. 1. Experimental setup used in the high-temperature AFM. The laser source is configured in the total internal reflection geometry to locally heat a deposited thin gold film.

<sup>a)</sup>Electronic mail: rsuper@physics.unc.edu

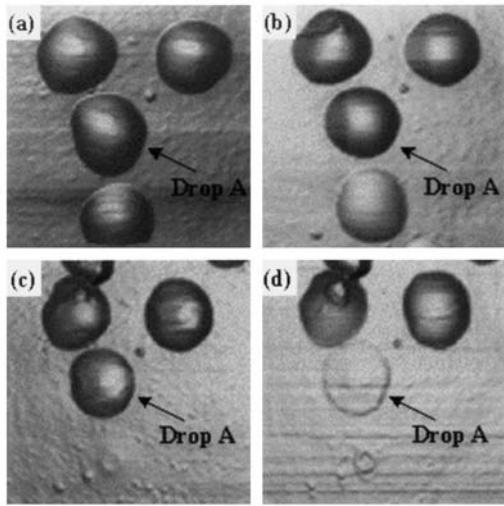


FIG. 2.  $6\ \mu\text{m}\times 6\ \mu\text{m}$  AFM images of four spheres taken at (a) 0 min, (b) 20 min, (c) 40 min, and (d) 60 min of irradiation. The spheres toward the bottom are flowing over time. Control experiments (not shown) comparing hot and cold images show the AFM to be a reliable imaging technique for the flowing polymer.

spheres with the laser on and off. The images differed only in the volume of the spheres, consistent with the thermal expansion of polystyrene. The temperature of the surface in the middle of the scan region was determined to be  $225\pm 5\ ^\circ\text{C}$  by comparing the spreading rate observed by the HT-AFM with those found from *ex situ* experiments using a calibrated oven. The *ex situ* measurements showed identical spreading behavior as the *in situ*, HT-AFM images.

A simple model can explain the time evolution of the spreading of the polymer drops. In Fig. 3, we plot the volume in drop A as a function of time. The line is a linear fit to the data. One possible model for this system is that of a droplet acting as a reservoir for a thin precursor film of constant thickness,  $e$ , which spreads out over the surface. The decreasing volume of the droplet is due to the spreading precursor film that drains the drop. Equating the change in the drop volume to the increase in the precursor film volume,  $V'_d = V'_f$ , we obtain  $V'_d = \pi D e$ , where the primes denote derivatives with respect to time. In obtaining this equation, we have assumed  $V_f = \pi l_f^2 e$ , with the spreading in the diffusive

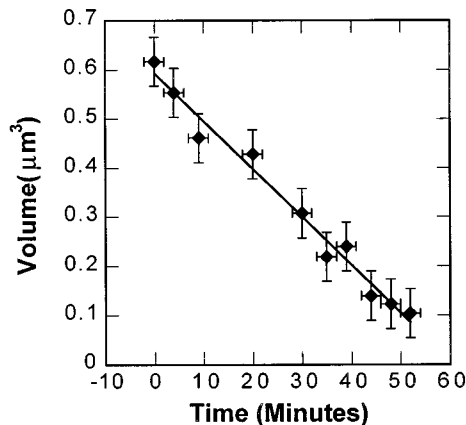


FIG. 3. Volume of sphere A as a function of irradiation time. The line is a linear fit of the data with the slope given by  $1.61\times 10^{-22}\ \text{m}^3/\text{s}$ .

regime,  $l_f = (Dt)^{1/2}$ , where  $D$  is the diffusion constant.<sup>6</sup> This model, therefore, accounts for the linear decrease of the drop volume.

Using this model, we can compare the derived  $V'_d = \pi D e$  with theoretical predictions for spreading polymer films. In one scenario, the diffusion constant,  $D$ , is related to the spreading parameter  $S = \gamma_s - (\gamma_{sl} + \gamma_l)$ , surface tension of spreading fluid  $\gamma_1$ , and its viscosity  $\eta$ , through  $D = \sqrt{2\gamma S/3(a/\eta)}$ , where  $a$  is given by the lateral dimension of the polymer. The film thickness is predicted to be  $e = a\sqrt{3\gamma/2S}$ .<sup>6</sup> Together, these two expressions yield  $V'_d = \pi a^2 \gamma/\eta$ . This is a convenient expression as it describes our experimentally-derived quantity without explicitly requiring the spreading parameter, which itself requires knowledge of the solid/ambient and solid/liquid surface energies,  $\gamma_s$  and  $\gamma_{sl}$ , respectively. These quantities are difficult to obtain experimentally. Our polystyrene beads have a large polydispersity index (molar mass distribution of 250–1000 kg/mol), with corresponding bulk viscosity  $\eta = (0.9\text{--}100)\times 10^4\ \text{Pa s}$  at  $217\ ^\circ\text{C}$ .<sup>7</sup> With  $\gamma_1 = 30\ \text{mJ}/\text{m}^2$ ,<sup>8</sup>  $a = 0.7\ \text{nm}$ , and taking the viscosity from the smallest molecular weight polymer fraction, the theory predicts  $V'_d = 5.1\times 10^{-24}\ \text{m}^3/\text{s}$ . This is at least two orders of magnitude smaller than the value obtained from the fit to the data of Fig. 3,  $V'_d = 1.61\pm 0.08\times 10^{-22}\ \text{m}^3/\text{s}$ . We expect that this discrepancy lies in our use of the bulk viscosity, which for our high molecular weights includes the effects of entanglements. If we assume that the molecular weight scaling of the viscosity is that appropriate for an unentangled melt, we obtain  $\eta = 1.5\times 10^3\ \text{Pa s}$  and  $V'_d = 3.1\times 10^{-23}\ \text{m}^3/\text{s}$ . This represents a good agreement with our experimental value considering that the viscosity values are reported for a temperature lower than that at which the experiment was conducted.

Why is the precursor film not evident in our images? The above expression for  $e = a\sqrt{3\gamma/2S}$  predicts that the precursor film should be less than 1 nm for surfaces of high surface energy, such as those of metals. This is confirmed by measurements of the polystyrene spreading on flat silicon substrates for which  $e = 0.7\ \text{nm}$ .<sup>9</sup> There is no corresponding data available for polymers on metals. This film thickness would be expected to be difficult to image on the relatively rough metal films used in these studies. Furthermore, it is possible that the polymer is spreading along the valleys of the film, making its detection even more difficult.

We have demonstrated an instrument that allows the application of atomic force microscopy to systems at elevated temperatures to  $225\ ^\circ\text{C}$ , with the potential of going to substantially higher temperatures. To the best of our knowledge, this is the highest reported temperature at which AFM has been performed in ambient. We have observed the spreading of polymer drops on gold at these elevated temperatures, and have shown the spreading behavior to be quantitatively consistent with a theoretical picture where the drop acts as a reservoir for a spreading precursor film. Future extensions of this work include establishing the high-temperature limits of this implementation and studying polymer flow under large temperature gradients.

The authors gratefully acknowledge support from the NSF HPCC program and the Hoechst Celanese Corporation.

- <sup>1</sup>*Forces in Scanning Probe Methods*, 1st ed., edited by H.-J. Guntherodt, D. Anselmetti, and E. Meyer (Kluwer Academic, Dordrecht, The Netherlands, 1995).
- <sup>2</sup>V. J. Novotny, *J. Chem. Phys.* **92**, 3189 (1990); P. G. deGennes, *Rev. Mod. Phys.* **57**, 827 (1985); J. Daillant, J. J. Benattar, and L. Leger, *Phys. Rev. A* **41**, 1963 (1990).
- <sup>3</sup>F. Heslot, A. Cazabat, and P. Levinson, *Phys. Rev. Lett.* **62**, 1286 (1989); J. Oliver and S. Mason, *J. Colloid Interface Sci.* **60**, 480 (1977).
- <sup>4</sup>G. Slak, I. Musevic, and R. Blinc, *Rev. Sci. Instrum.* **67**, 2554 (1996).
- <sup>5</sup>H. J. Mamin, *Appl. Phys. Lett.* **69**, 433 (1996).
- <sup>6</sup>J. F. Joanny and P. G. deGennes, *J. Phys. (Paris)* **47**, 121 (1986).
- <sup>7</sup>T. G. Fox and P. J. Flory, *J. Polym. Sci.* **14**, 315 (1954).
- <sup>8</sup>Souheng Wu, *Polymer Interface and Adhesion*, 1st ed. (Marcel Dekker, New York, 1982), pp. 62 and 72.
- <sup>9</sup>P. Thiansathaporn, C.-H. Chen, D. Glick, and R. Superfine (unpublished data).